# New results on charmonium physics from BaBar.

Antimo Palano

*INFN and University of Bari*

*Representing the BABAR Collaboration*

## Summary

- Dalitz plot Analysis of $\eta_c \to K^+K^-\eta$ and $\eta_c \to K^+K^-\pi^0$ in two-photon interactions.
- Search for new resonances in $B \to J/\psi\,\phi K$ decays.

Workshop on Unquenched Hadron Spectroscopy:
Non-Perturbative Models and Methods of QCD vs. Experiment
15 September 2014 at the University of Coimbra, Portugal
Coimbra, September 2, 2014

## Study of $K^+K^-\eta$ and $K^+K^-\pi^0$ final states in two photon interactions.

□ Many $\eta_c$ and $\eta_c(2S)$ decays are still missing or studied with low statistics.

□ We make use of two-photon interactions to produce charmonium states.

□ We select events in which the $e^+$ and $e^-$ beam particles are scattered at small angles and are undetected in the detector.

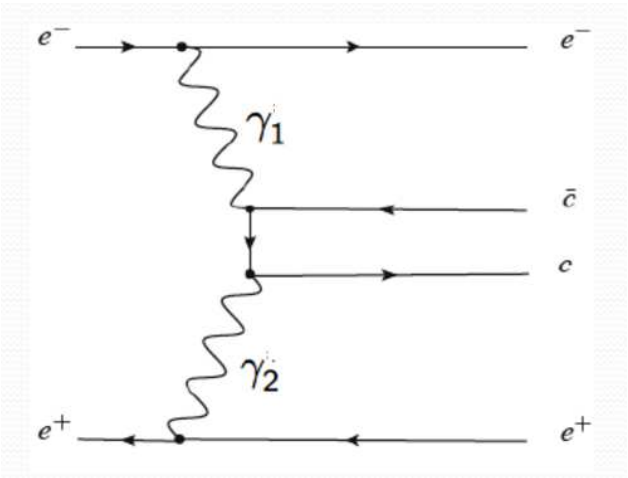


□ This implies that only resonances with $J^{PC} = 0^{\pm+}, 2^{\pm+}, 3^{++}, 4^{\pm+}$.... can be produced.

□ In addition the $K^+K^-\eta$ and $K^+K^-\pi^0$ states cannot be in a $J^P = 0^+$ state.

## Physics Motivations.

□ No Dalitz analysis has been ever published on $\eta_c$ ($J^{PC} = 0^{-+}$) three-body decays.

□ Low mass charmonium states decay predominantly to multi-body light mesons final states, and thus offer great opportunities for studying light meson spectroscopy.

□ $\eta_c$ decays are useful for obtaining new information on the scalar mesons.

□ It is interesting therefore to look at $\eta_c$ decays.

□ In this analysis we study the following two-photon production processes (arXiv:1403.7051):

$$\gamma\gamma \to K^+K^-\eta$$

$$\to \gamma\gamma$$

$$\to \pi^+\pi^-\pi^0$$

$$\gamma\gamma \to K^+K^-\pi^0$$

## Data selection.

□ For each final state we select events having the exact number of expected charged tracks.

□ Due to soft photons background we allow the presence of extra low energy $\gamma$'s.

□ We select two-photon events by requiring the conservation of the transverse momentum $p_T$. We require $p_T < 0.05$ GeV/c

□ $p_T$ distributions for the three reactions.

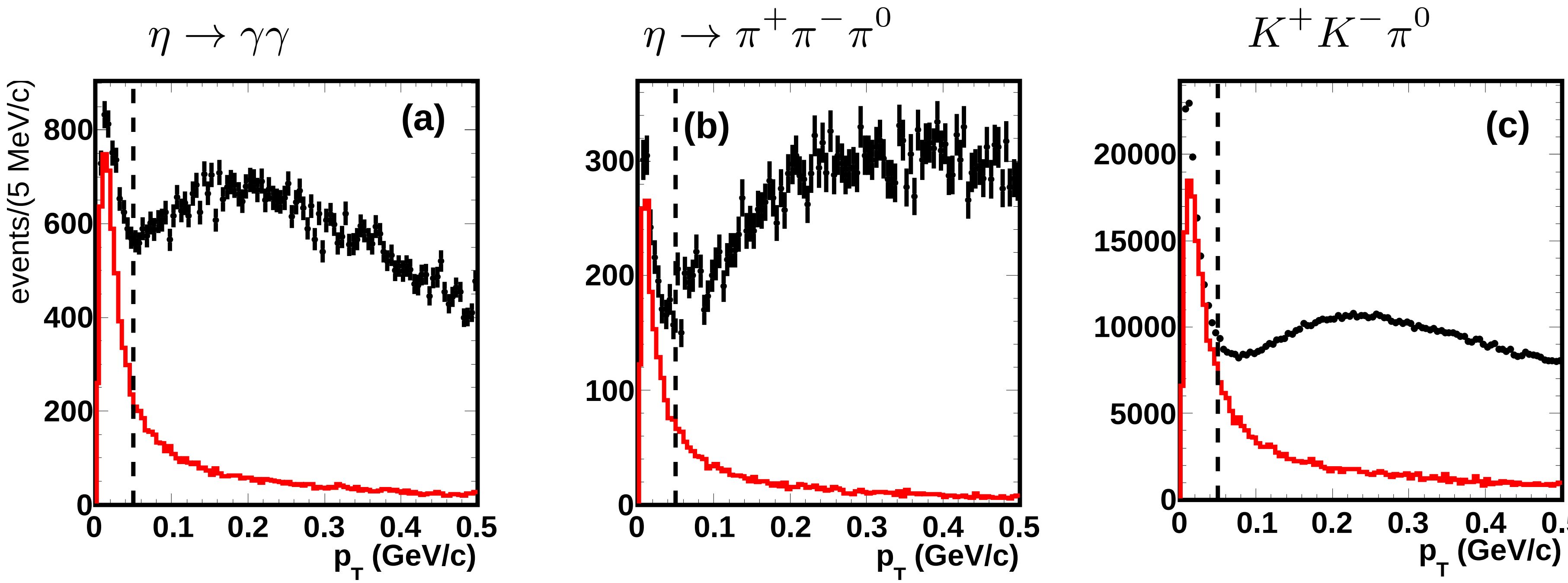


□ Good agreement with MC simulations.

## Experimental resolution.

☐ We make use of MC simulations to obtain the experimental resolution for each channel.

☐ Resolution functions fitted with the sum of a Crystal Ball and a Gaussian function.

$\eta \to \gamma\gamma$ $\eta \to \pi^+\pi^-\pi^0$ $K^+K^-\pi^0$

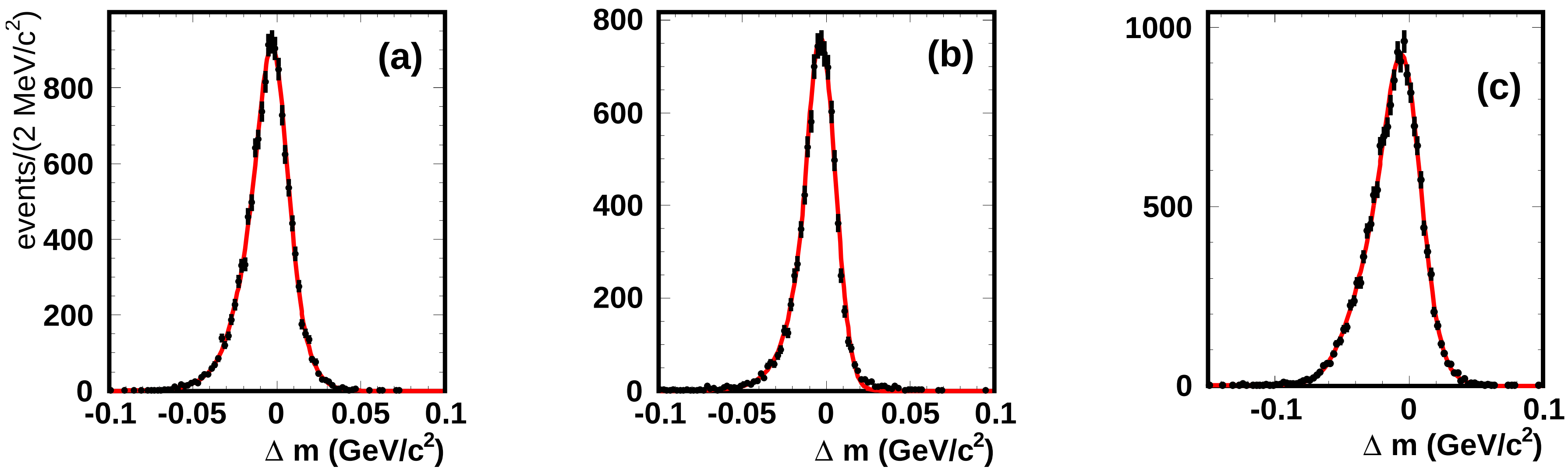


☐ r.m.s. values at the $\eta_c$ mass are 15, 14, and 21 MeV/$c^2$.

## $\eta K^+ K^-$ mass spectra

□ Mass spectra for the two $\eta$ decay modes.

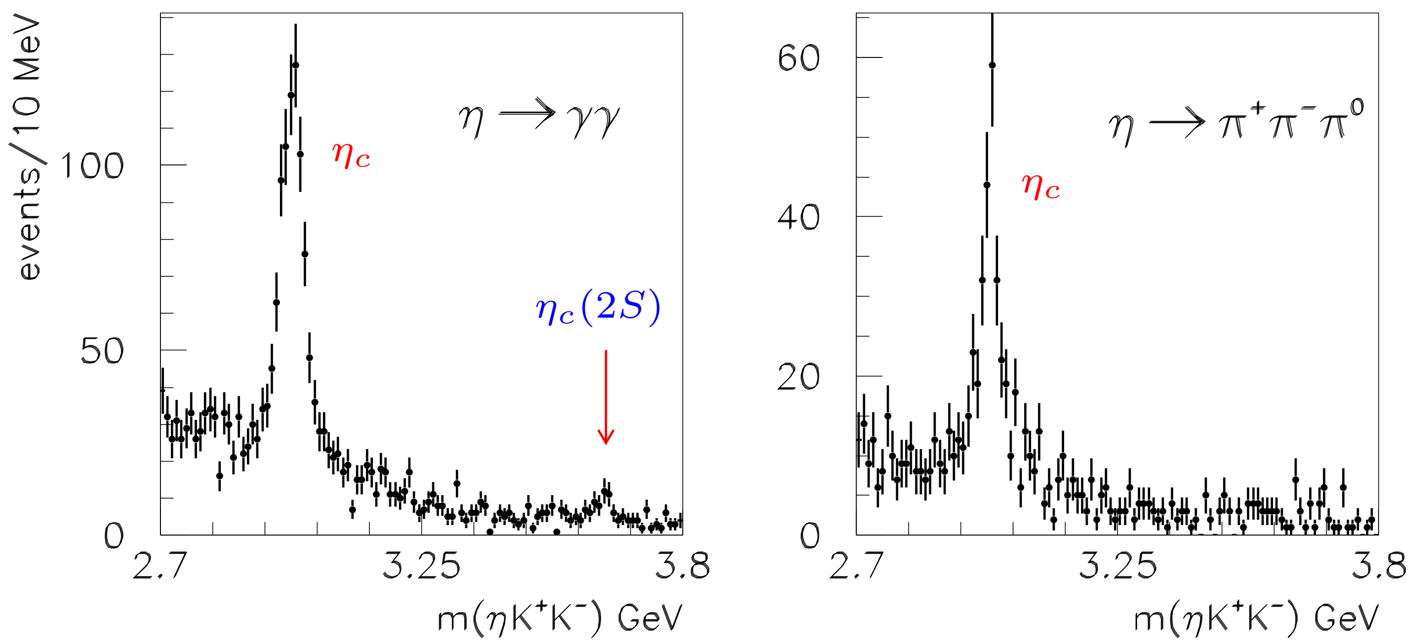


□ Strong $\eta_c$ and some $\eta_c(2S)$ signal. First observations.

# Mass spectra.

□ $K^+K^-\eta$ mass spectrum summed over the two $\eta$ decay modes and and $K^+K^-\pi^0$ mass spectrum.

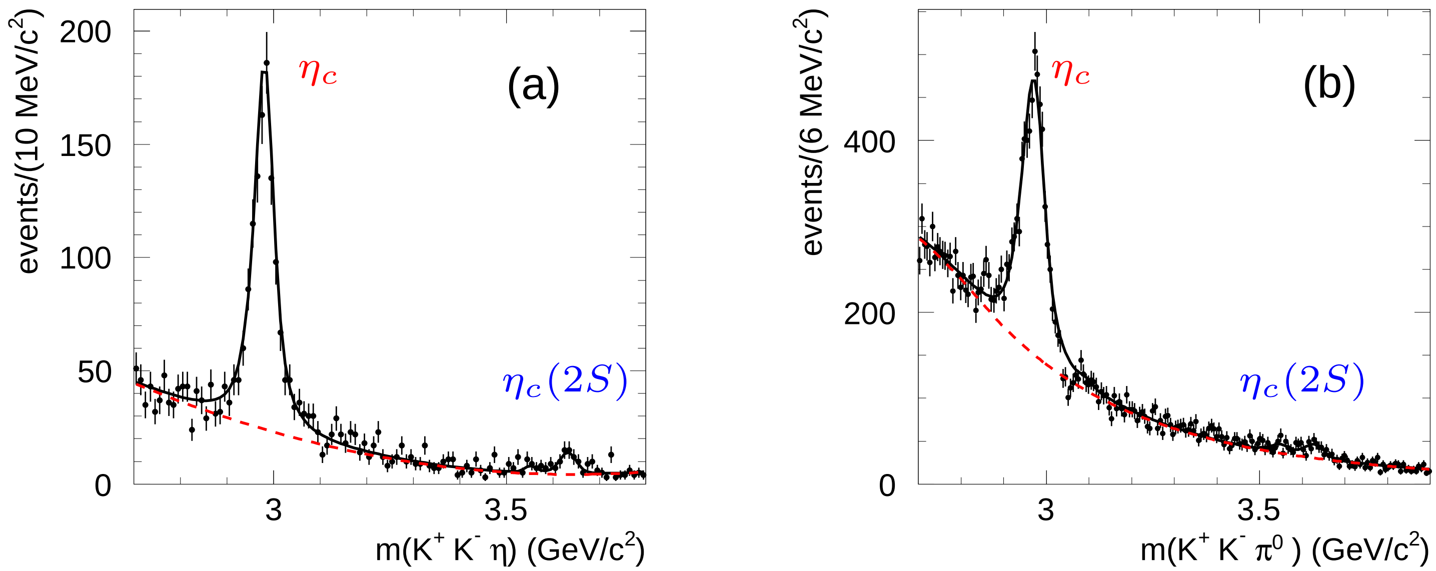


□ Strong $\eta_c$ signals. Evidence for $\eta_c(2S)$ and $\chi_{c2}$. Small $J/\psi$ signal from residual ISR background.

□ Charmonium signals fitted using Breit-Wigner functions convolved with the resolution functions.

# Efficiency.

□ Fitted detection efficiency in the $\cos\theta$ *vs.* $m(K^+K^-)$ plane, where $\theta$ is the $K^+$ helicity angle.

□ Efficiency distributions for the three reactions in the $\eta_c$ mass region.

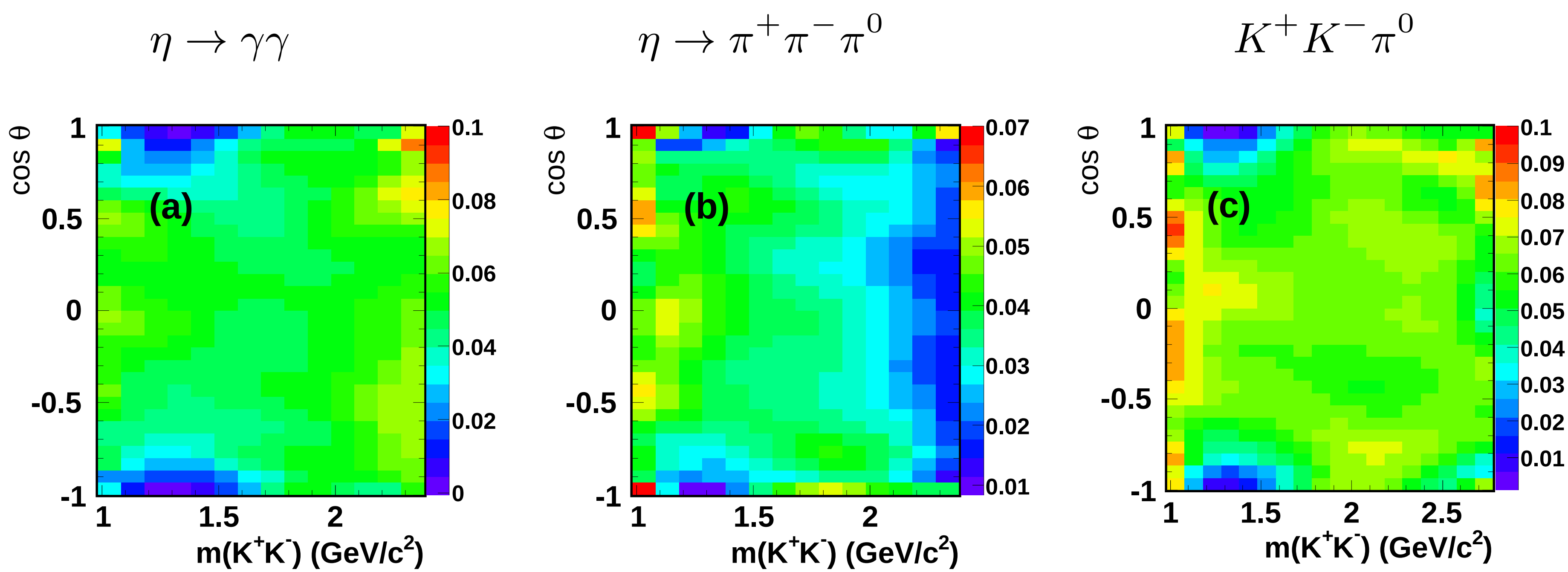


□ Efficiency fitted using Legendre polynomials moments.

□ Some efficiency loss due to low momentum kaons or $\pi^0$.

## Fitted masses.

| Resonance | Mass ( MeV/$c^2$) | $\Gamma$ (MeV) |
|---|---|---|
| $\eta_c \to K^+K^-\eta$ | $2984.1 \pm 1.1 \pm 2.1$ | $34.8 \pm 3.1 \pm 4.0$ |
| $\eta_c \to K^+K^-\pi^0$ | $2979.8 \pm 0.8 \pm 3.5$ | $25.2 \pm 2.6 \pm 2.4$ |
| $\eta_c(2S) \to K^+K^-\eta$ | $3635.1 \pm 5.8 \pm 2.1$ | 11.3 (fixed) |
| $\eta_c(2S) \to K^+K^-\pi^0$ | $3637.0 \pm 5.7 \pm 3.4$ | 11.3 (fixed) |

- Event yields and significances for the charmonium states.

| Channel | Event yield | Significance |
|---|---|---|
| $\eta_c \to K^+K^-\pi^0$ | $4518 \pm 131 \pm 50$ | $32\ \sigma$ |
| $\eta_c \to K^+K^-\eta\ (\eta \to \gamma\gamma)$ | $853 \pm 38 \pm 11$ | $21\ \sigma$ |
| $\eta_c \to K^+K^-\eta\ (\eta \to \pi^+\pi^-\pi^0)$ | $292 \pm 20 \pm 7$ | $14\ \sigma$ |
| $\eta_c(2S) \to K^+K^-\pi^0$ | $178 \pm 29 \pm 39$ | $3.7\ \sigma$ |
| $\eta_c(2S) \to K^+K^-\eta$ | $47 \pm 9 \pm 3$ | $4.9\ \sigma$ |
| $\chi_{c2} \to K^+K^-\pi^0$ | $88 \pm 27 \pm 23$ | $2.5\ \sigma$ |
| $\chi_{c2} \to K^+K^-\eta$ | $2 \pm 5 \pm 2$ | $0.0\ \sigma$ |

## Branching fractions.

□ We compute the ratios of the branching fractions for $\eta_c$ and $\eta_c(2S)$ decays to the $K^+K^-\eta$ final state compared to the respective branching fractions to the $K^+K^-\pi^0$ final state.

$$\mathcal{R} = \frac{\mathcal{B}(\eta_c/\eta_c(2S) \to K^+K^-\eta)}{\mathcal{B}(\eta_c/\eta_c(2S) \to K^+K^-\pi^0)} = \frac{N_{K^+K^-\eta}}{N_{K^+K^-\pi^0}} \frac{\epsilon_{K^+K^-\pi^0}}{\epsilon_{K^+K^-\eta}} \frac{1}{\mathcal{B}_\eta}$$

□ Presence of non-negligible backgrounds in the $\eta_c$ signals, which have different distributions in the Dalitz plot

□ We perform a sideband subtraction by assigning a weight $w = 1/\epsilon(m, \cos\theta)$ to events in the signal region and a negative weight $w = -f/\epsilon(m, \cos\theta)$ to events in the sideband regions.

□ The weight in the sideband regions is scaled down by the factor $f$ to match the fitted $\eta_c$ signal/background ratio.

□ We obtain the weighted efficiencies as

$$\epsilon_{K^+K^-\eta/\pi^0} = \frac{\sum_{i=1}^{N} f_i}{\sum_{i=1}^{N} f_i/\epsilon(m_i, \cos\theta_i)}$$

where $N$ indicates the number of events in the signal+sidebands regions.

## Branching fractions.

□ We obtain:

$$\mathcal{R}(\eta_c) = \frac{\mathcal{B}(\eta_c \to K^+K^-\eta)}{\mathcal{B}(\eta_c \to K^+K^-\pi^0)} = 0.571 \pm 0.025 \pm 0.051$$

□ Consistent with the BESIII measurement of $0.46 \pm 0.23$ ($6.7 \pm 3.2$ events for $\eta_c \to K^+K^-\eta$) (Phys.Rev. D **86**, 092009 (2012).

□ We also obtain:

$$\mathcal{R}(\eta_c(2S)) = \frac{\mathcal{B}(\eta_c(2S) \to K^+K^-\eta)}{\mathcal{B}(\eta_c(2S) \to K^+K^-\pi^0)} = 0.82 \pm 0.21 \pm 0.27$$

# Dalitz plots.

- ☐ $\eta_c \to \eta K^+ K^-$ Dalitz plot. 1161 events with $(76.1 \pm 1.3)\%$ purity.
- ☐ Evidence for $f_0(1500)$, $f_0(1710)$ and $K_0^*(1430)$.

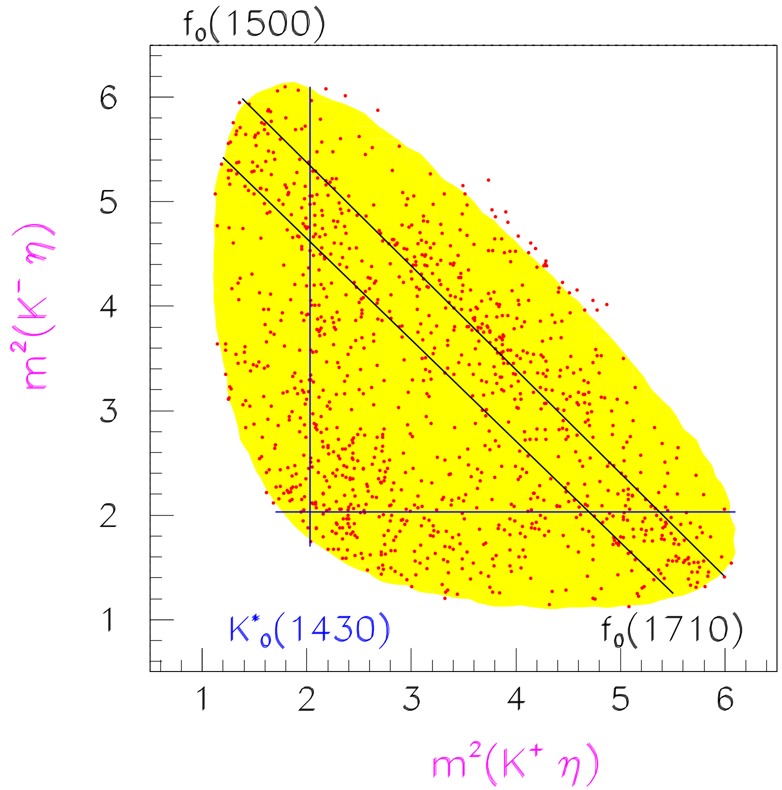


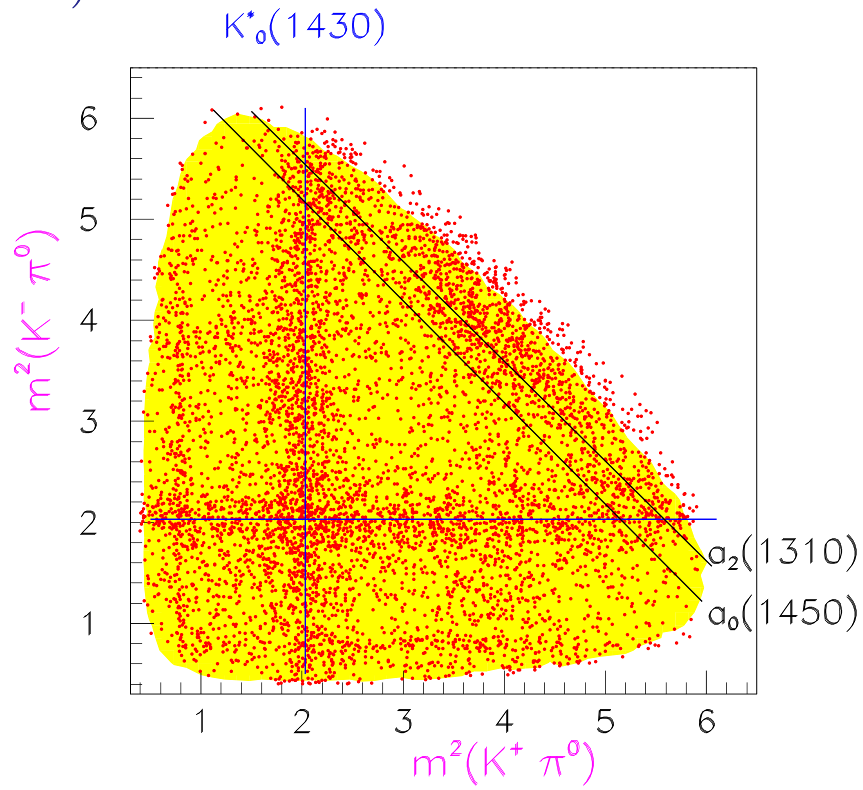


- ☐ $\eta_c \to \pi^0 K^+ K^-$ Dalitz plot. 6710 events with $(55.2 \pm 0.6)\%$ purity.
- ☐ Evidence for $a_0(980)$, $a_0(1450)$, $a_2(1310)$ and $K_0^*(1430)$.
- ☐ $K^*(890)$ mostly from background.

## Dalitz plot analysis.

- Unbinned Maximum Likelihood fit.
- Amplitudes parametrized as in a standard *pseudoscalar* $\rightarrow$ *three pseudoscalars* Dalitz analysis.
- Full interference allowed among the amplitudes.
- No evidence for interference between signal and background. Therefore the sidebands fitted using the sum of incoherent resonances.
- Background in the signal region estimated interpolating the sidebands.
- A Non-Resonant contribution $(NR)$ is included in the fit.
- The fit quality is tested by dividing the Dalitz plot in $N_{cells}$ cells and computing:

$$\chi^2 = \sum_{i=1}^{N_{cells}} (N^i_{obs} - N^i_{exp})^2 / N^i_{exp}$$

where $N^i_{obs}$ and $N^i_{exp}$ are event yields from data and simulation, respectively. Denoting by $n$ the number of free parameters in the fit, we label $\nu = N_{cells} - n$.

# $\eta_c \to \eta K^+ K^-$ Dalitz plot analysis.

□ Results from the Dalitz analysis and fit projections.

□ Charge conjugated amplitudes symmetrized.

| Final state | Fraction % | Phase (radians) |
|---|---|---|
| $f_0(1500)\eta$ | 23.7 ± 7.0 ± 1.8 | 0. |
| $f_0(1710)\eta$ | 8.9 ± 3.2 ± 0.4 | 2.2 ± 0.3 ± 0.1 |
| $f_0(2200)\eta$ | 11.2 ± 2.8 ± 0.5 | 2.1 ± 0.3 ± 0.1 |
| $f_0(1350)\eta$ | 5.0 ± 3.7 ± 0.5 | 0.9 ± 0.2 ± 0.1 |
| $f_0(980)\eta$ | 10.4 ± 3.0 ± 0.5 | -0.3 ± 0.3 ± 0.1 |
| $f_2'(1525)\eta$ | 7.3 ± 3.8 ± 0.4 | 1.0 ± 0.1 ± 0.1 |
| $K_0^*(1430)^+K^-$ | 16.4 ± 4.2 ± 1.0 | 2.3 ± 0.2 ± 0.1 |
| $K_0^*(1950)^+K^-$ | 2.1 ± 1.3 ± 0.2 | -0.2 ± 0.4 ± 0.1 |
| $NR$ | 15.5 ± 6.9 ± 1.0 | -1.2 ± 0.4 ± 0.1 |
| Sum | 100.0 ± 11.2 ± 2.5 | |
| $\chi^2/\nu$ | 87/65 | |

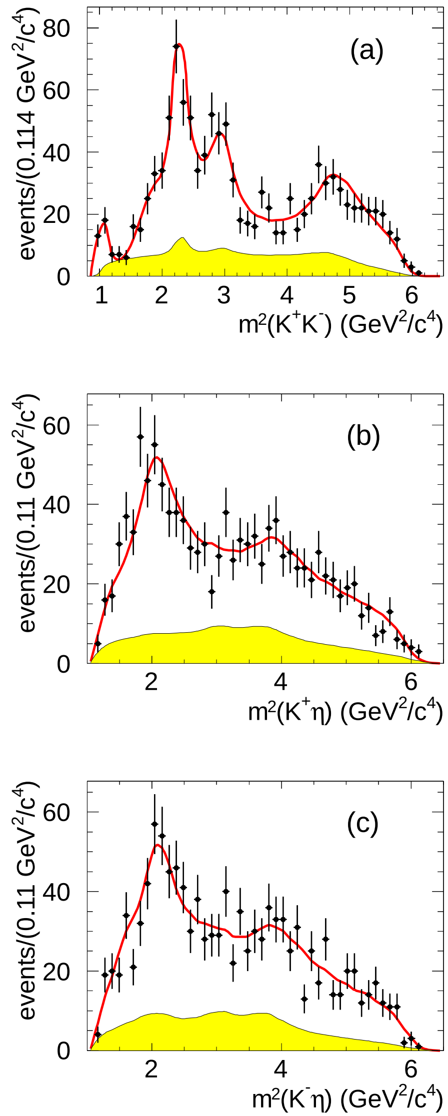


□ Largest amplitudes are $f_0(1500)\eta$ and $K_0^*(1430)K$.

□ The description of the data is adequate.

## $\eta_c \to \pi^0 K^+ K^-$ Dalitz analysis.

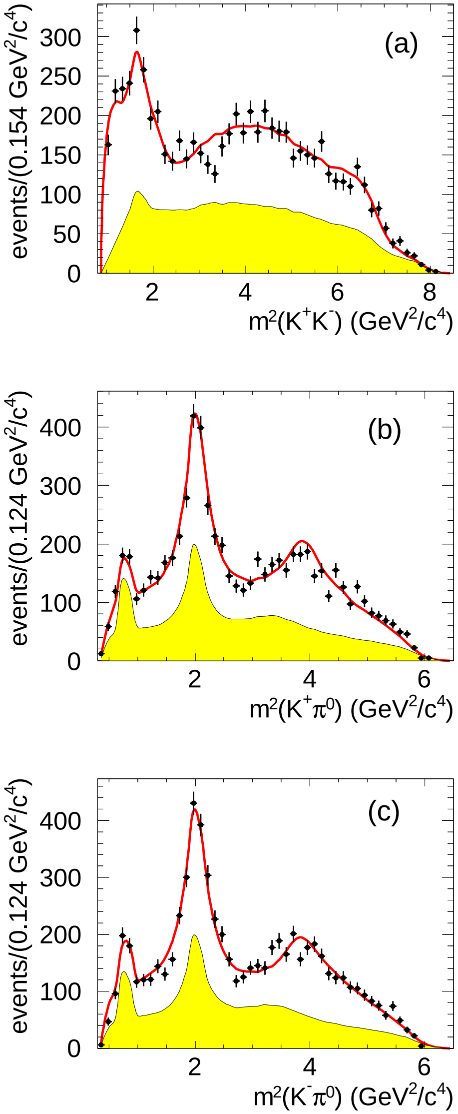


- Results from the Dalitz analysis and fit projections.

| Final state | Fraction % | Phase (radians) |
|---|---|---|
| $K_0^*(1430)^+K^-$ | $33.8 \pm 1.9 \pm 0.4$ | 0. |
| $K_0^*(1950)^+K^-$ | $6.7 \pm 1.0 \pm 0.3$ | $-0.67 \pm 0.07 \pm 0.03$ |
| $K_2^*(1430)^+K^-$ | $6.8 \pm 1.4 \pm 0.3$ | $-1.67 \pm 0.07 \pm 0.03$ |
| $a_0(980)\pi^0$ | $1.9 \pm 0.1 \pm 0.2$ | $0.38 \pm 0.24 \pm 0.02$ |
| $a_0(1450)\pi^0$ | $10.0 \pm 2.4 \pm 0.8$ | $-2.4 \pm 0.05 \pm 0.03$ |
| $a_2(1320)\pi^0$ | $2.1 \pm 0.1 \pm 0.2$ | $0.77 \pm 0.20 \pm 0.04$ |
| $NR$ | $24.4 \pm 2.5 \pm 0.6$ | $1.49 \pm 0.07 \pm 0.03$ |
| Sum | $85.8 \pm 3.6 \pm 1.2$ | |
| $\chi^2/\nu$ | 212/130 | |

- Largest amplitudes are $K_0^*(1430)K$ and $a_0(1450)\pi^0$.
- $K_1^*(890)K$ amplitude consistent with zero.
- Spin-one resonances consistent to originate entirely from background.
- Some residual background from $\gamma\gamma \to K^+K^-$.
- The isobar model does not fit very well the data.

## The $K_0^*(1430)$ parameters.

□ In the $\eta_c \to \pi^0 K^+ K^-$ Dalitz plot analysis we scan the likelihood as a function of the $K_0^*(1430)$ mass and width.

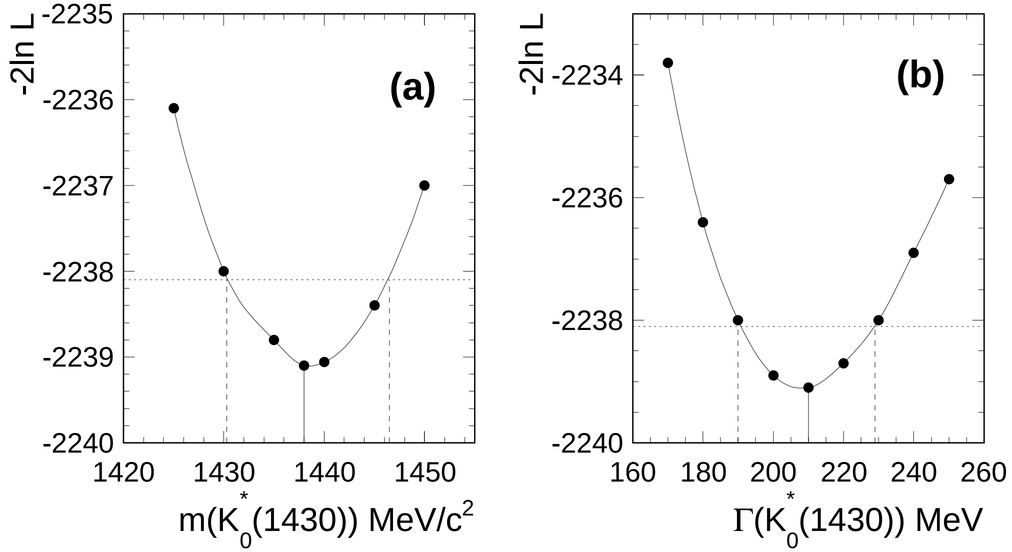


□ We obtain:

$$m(K_0^*(1430)) = 1438 \pm 8 \pm 4 \ \text{MeV}/c^2$$

$$\Gamma(K_0^*(1430)) = 210 \pm 20 \pm 12 \ MeV$$

## $K_0^*(1430)$ branching fraction.

☐ First observation of $K_0^*(1430) \to K\eta$.

☐ The observation of $K_0^*(1430)$ in both $K\eta$ and $K\pi^0$ decay modes allows a measurement of the relative branching fraction.

☐ The Dalitz plot analysis of $\eta_c \to K^+K^-\eta$ decay gives a total $K_0^*(1430)^+K^-$ contribution of

$$f_{\eta K} = 0.164 \pm 0.042 \pm 0.010$$

☐ The Dalitz plot analysis of the $\eta_c \to K^+K^-\pi^0$ decay mode gives a total $K_0^*(1430)^+K^-$ contribution of

$$f_{\pi^0 K} = 0.338 \pm 0.019 \pm 0.004$$

☐ Using the measurement of $\mathcal{R}(\eta_c)$, we obtain the $K_0^*(1430)$ branching ratio

$$\frac{\mathcal{B}(K_0^*(1430) \to \eta K)}{\mathcal{B}(K_0^*(1430) \to \pi K)} = \mathcal{R}(\eta_c)\frac{f_{\eta K}}{f_{\pi K}} = 0.092 \pm 0.025^{+0.010}_{-0.025}$$

where $f_{\pi K}$ denotes $f_{\pi^0 K}$ after correcting for the $K^0\pi$ decay mode.

☐ Asymmetric systematic uncertainty.

## $K_0^*(1430)$ branching fraction.

□ We note that the amplitude labelled "$NR$" may be considered to represent an $\mathcal{S}$-wave, similar to that of the $K_0^*(1430)^+K^-$ amplitudes

□ We remove the non-resonant contribution in both the $\eta_c \to K^+K^-\eta$ and $\eta_c \to K^+K^-\pi^0$ Dalitz plot analyses.

□ We obtain significant variation of the $K_0^*(1430)^+K^-$ fraction in the $\eta_c \to K^+K^-\pi^0$ final state ($\approx$ a factor 2) which is included in the evaluation of the systematic uncertainty.

□ The LASS experiment studied the reaction $K^-p \to K^-\eta p$ at 11 GeV/$c$. The $K^-\eta$ mass spectrum is dominated by the presence of the $K_3^*(1780)$ resonance with no evidence for $K_0^*(1430) \to K\eta$ decay.

□ However, from PDG:

$$\Gamma(K_0^*(1430) \to K\pi)/\Gamma(K_0^*(1430)) = 0.93 \pm 0.04 \pm 0.09$$

□ Not in conflict with the presence of a small branching fraction for the $K\eta$ decay mode.

## Implications for the pseudoscalar meson mixing angle.

□ No evidence for $K_0^*(1430)$ or $K_2^*(1430)$ production in the reaction $K^-p \to K^-\eta p$ at 11 by LASS experiment with an upper limit

$$\mathcal{B}(K_2^*(1430) \to K\eta)/\mathcal{B}(K_2^*(1430) \to K\pi) < 0.92\% \ at \ 95\% \ C.L.$$

□ This small value is understood in the context of an SU(3) model with octet-singlet mixing of the $\eta$ and $\eta'$.

□ For even angular momentum $l$ (i.e., D-type coupling), it can be shown that a consequence of the resulting $K^*\bar{K}\eta$ couplings is

$$R_l = \frac{\mathcal{B}(K_l^* \to K\eta)}{\mathcal{B}(K_l^* \to K\pi)} = \frac{1}{9}(\cos\theta_p + 2\cdot\sqrt{2}\cdot\sin\theta_p)^2 \cdot (q_{K\eta}/q_{K\pi})^{2l+1}$$

where $q_{K\eta}$ ($q_{K\pi}$) is the kaon momentum in the $K\eta$ ($K\pi$) rest frame at the $K^*$ mass and $\theta_p$ is the SU(3) singlet-octet mixing angle for the pseudoscalar meson nonet.

□ We note that $R_l$ equals zero if

$$\tan\theta_p = -[1/(2\cdot\sqrt{2})](i.e., \theta_p = -19.7^\circ)$$

## Implications for the pseudoscalar meson mixing angle.

□ For $l = 2$, the upper limit $R_2 = 0.0092$ corresponds to $\theta_p = -9.0^\circ$ and the central value yields $\theta_p = -11.4^\circ$.

□ In the present analysis, we obtain the value $R_0 = 0.092^{+0.027}_{-0.035}$.

□ The corresponding value of $\theta_p$ is:

$$\theta_p = (3.1^{+3.3}_{-5.0})^\circ$$

which differs by about 2.9 standard deviations from the result obtained from the $K_2^*(1430)$ branching ratio.

□ However, in Feldmann et al. (Int. J. Mod. Phys. A **15**, 159 (2000)), it is argued that it is necessary to consider separate octet and singlet mixing angles for the pseudoscalar mesons.

## Search for resonances decaying to $J/\psi\,\phi$.

□ Several experiments, CDF, CMS and D0 observe structures in the $J/\psi\,\phi$ mass spectrum from $B^+ \to J/\psi\phi K^+$.

□ An early study from LHCb do no confirm these findings.

□ The interest is that these resonances may be some type of multiquark states.

□ $J/\psi\,\phi$ mass spectrum from CMS.

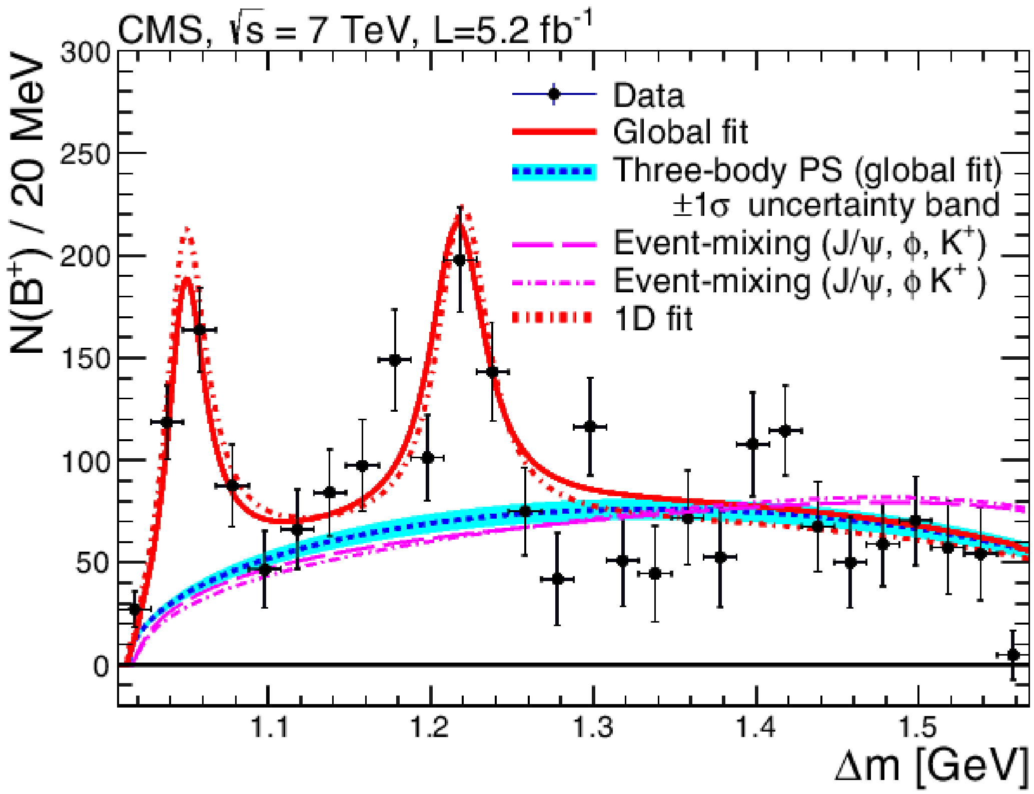


$$\Delta m = m(\mu^+\mu^- K^+ K^-) - m(\mu^+\mu^-)$$

## A summary of experimental results.

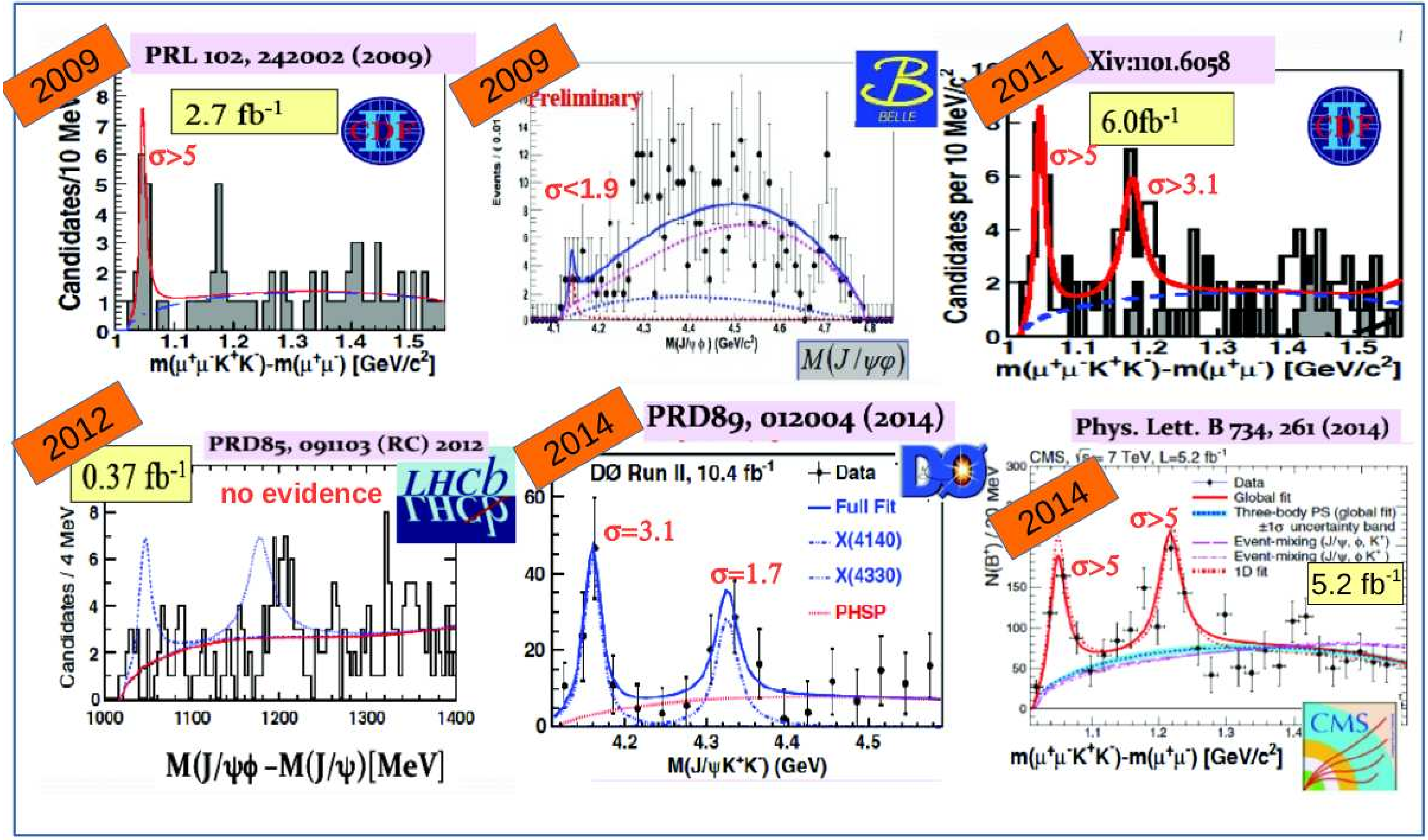

# Search for resonances decaying to $J/\psi K^+K^-$ in $B$ meson decay.

- Use of the full *BABAR* $\Upsilon(4S)$ dataset, 424 $fb^{-1}$ (arXiv:1407.7244) (charge conjugation is implied).
- We study the reactions $B^+ \to J/\psi K^+K^-K^+$ and $B^0 \to J/\psi K^+K^-K^0_S$.
- $\Delta E$ signals after requiring $m_{ES} > 5.27\,\mathrm{GeV}/c^2$.

$\Delta E \equiv E^*_B - \sqrt{s}/2,$

$m_{ES} \equiv \sqrt{((s/2 + \vec{p}_i \cdot \vec{p}_B)/E_i)^2 - \vec{p}^{\,2}_B},$

$(E_i, \vec{p}_i)$ is the initial state $e^+e^-$ four-momentum vector in the lab. and $\sqrt{s}$ is the c.m. energy.
$E^*_B$ is the $B$ meson energy in the c.m., $\vec{p}_B$ is its lab. momentum.

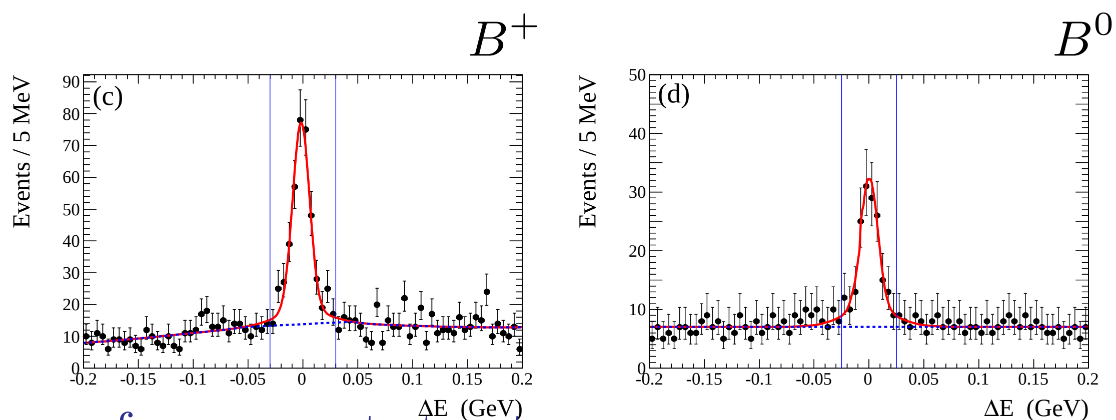


- $J/\psi K^+K^-$ mass spectra. No evidence for resonant structures.

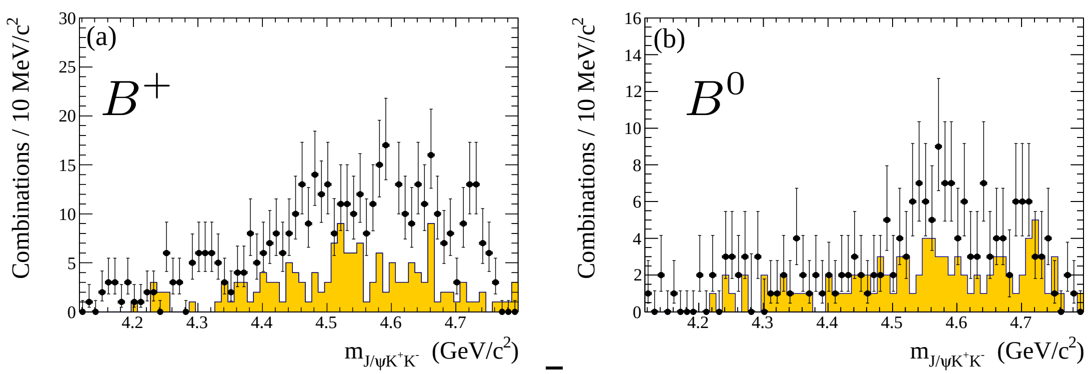

# Selection of $B \to J/\psi\,\phi K$.

- $K^+K^-$ mass spectra for $B^+ \to J/\psi K^+K^-K^+$ and $B^0 \to J/\psi K^+K^-K^0_S$.
- Clear $\phi$ signals.

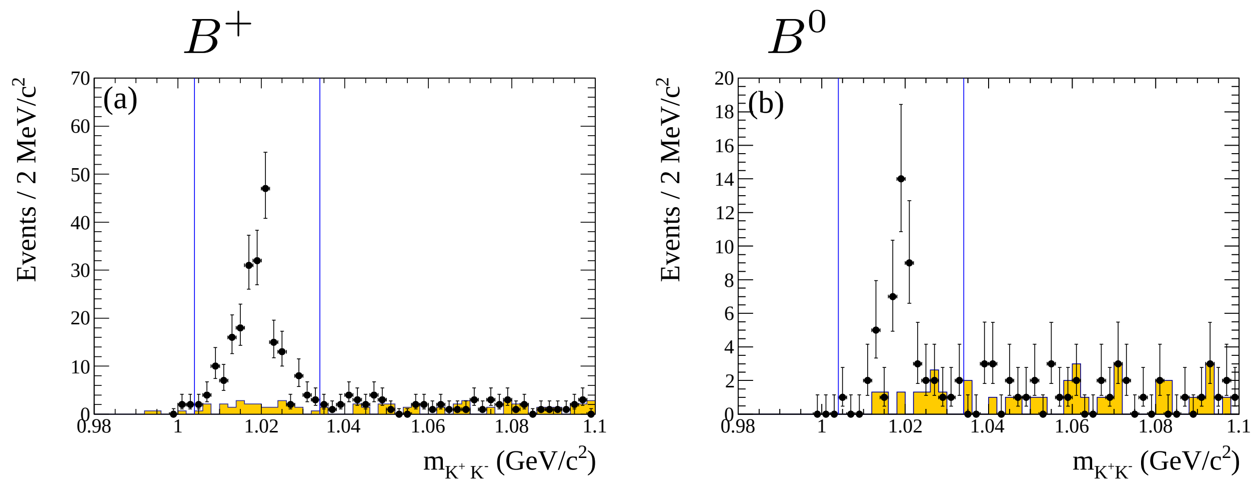


- Selecting a $\phi$ signal we obtain the corresponding $\Delta E$ distributions.

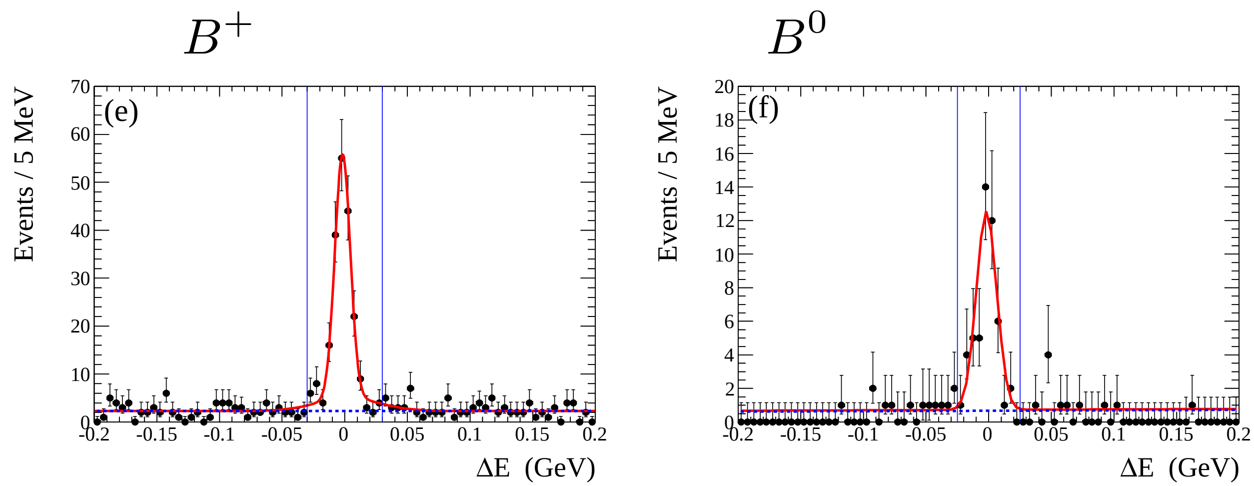

## Branching fractions.

- $J/\psi\, X$ yields and branching fractions.
- Each event is weighted by the inverse of the efficiency on the Dalitz plot.

| $B$ channel | Event yield | $\mathcal{B}$ $(\times 10^{-5})$ |
|---|---|---|
| $B^{+}{}_{KKK}$ | 290±22 | 6.91±0.52 (stat)±0.28 (sys) |
| $B^{+}_{\phi K}$ | 189±1 | 5.06±0.37 (stat)±0.15 (sys) |
| $B^{0}{}_{KKK_S}$ | 68±13 | 3.35±0.66 (stat)±0.15 (sys) |
| $B^{0}{}_{\phi K_S}$ | 41± 7 | 2.13±0.36 (stat)±0.06 (sys) |
| $B^{0}{}_{\phi}$ | 6 ± 4 | $< 0.101$ |

- $\Delta E$ signal for $B^0 \to J/\psi\phi$ candidates: no signal.

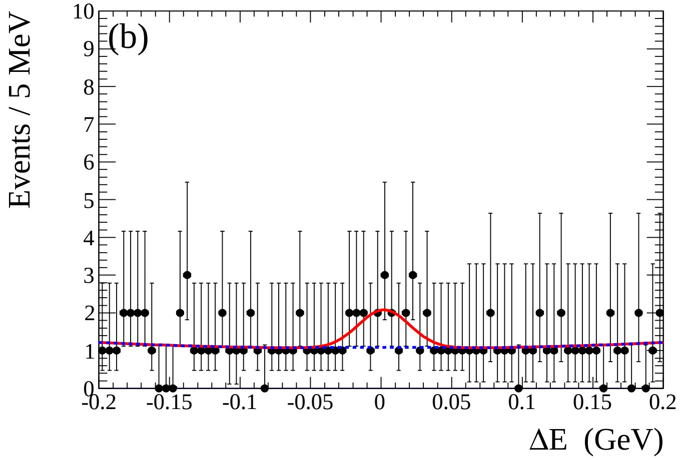

## Branching fractions.

- We compute the ratios:

$$R_+ = \frac{\mathcal{B}(B^+ \to J/\psi K^+K^-K^+)}{\mathcal{B}(B^+ \to J/\psi \phi K^+)} = 1.39 \pm 0.15 \pm 0.07$$

$$R_0 = \frac{\mathcal{B}(B^0 \to J/\psi K^+K^-K^0_S)}{\mathcal{B}(B^0 \to J/\psi \phi K^0_S)} = 1.54 \pm 0.40 \pm 0.08$$

and they are consistent with being equal within the uncertainties.

- For the ratios:

$$R_\phi = \frac{\mathcal{B}(B^0 \to J/\psi \phi K^0_S)}{\mathcal{B}(B^+ \to J/\psi \phi K^+)} = 0.48 \pm 0.09 \pm 0.02$$

$$R_{2K} = \frac{\mathcal{B}(B^0 \to J/\psi K^+K^-K^0_S)}{\mathcal{B}(B^+ \to J/\psi K^+K^-K^+)} = 0.52 \pm 0.09 \pm 0.03$$

we find values in agreement with the expectation of the spectator quark model ($R_\phi \sim R_{2K} \sim 0.5$).

# Efficiency.

□ We compute the efficiency on the Dalitz plot by generating and reconstructing phase space MC events.

□ Efficiency on the Dalitz plot for $B^+ \to J/\psi\phi K^+$ and $B^0 \to J/\psi\phi K^0_S$.

$B^+$ $B^0$

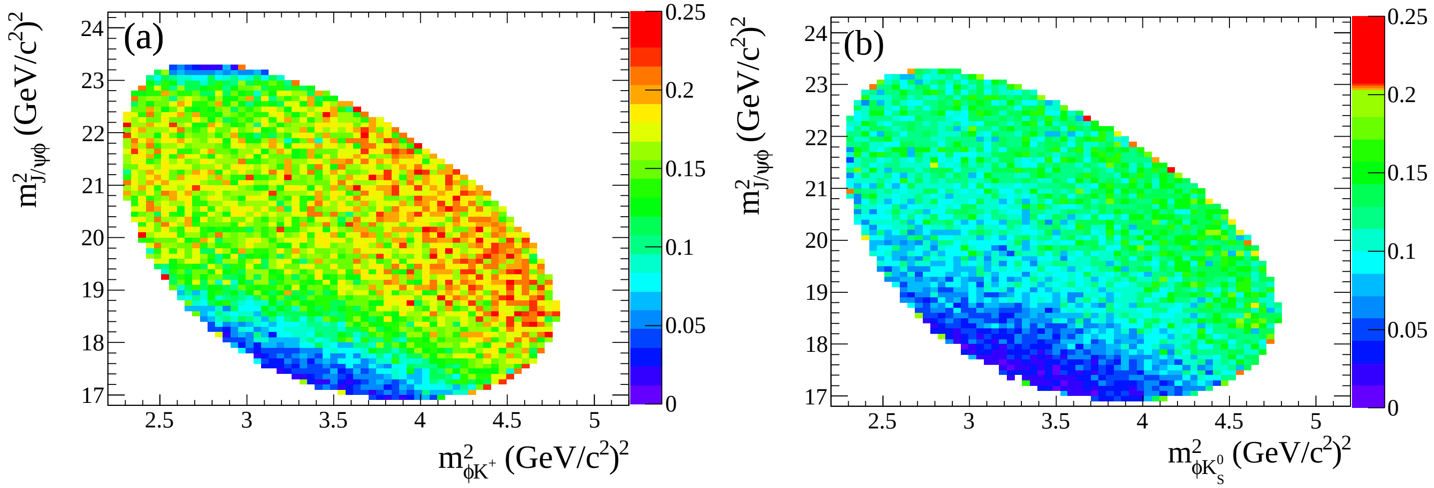


□ The lower efficiency at low $J/\psi\phi$ mass is due to the lower reconstruction of low kaon momentum in the laboratory frame, as a result of energy loss in the beampipe and SVT material.

## Search for resonances in the $J/\psi\phi$ mass spectra.

□ We search for the resonances claimed by the CDF collaboration by performing an unbinned maximum likelihood fit for $B \to J/\psi\phi K$ decays.

- We model the resonances using S-wave relativistic Breit-Wigner functions with parameters fixed to the CDF values.
- The non-resonant contributions are represented by a constant term (PHSP) and no interference is allowed between the fit components.
- We estimate the background contributions from the $\Delta E$ sidebands and incorporated into the non-resonant PHSP term.
- The decay of a pseudoscalar meson to two vector states contains high spin contributions which could generate non-uniform angular distributions.
- However, due to the limited data sample we do not include such angular terms, and assume that the resonances decay isotropically.
- The amplitudes are normalized using PHSP MC generated events.
- The fit functions are weighted by the the two-dimensional efficiency computed on the Dalitz plots.

## Search for resonances in the $J/\psi\phi$ mass spectra.

□ Fit projections on the $J/\psi\phi$ mass spectra in the hypothesis of the presence of two $X(4140)$ and $X(4270)$ resonances.

$B^+$ $B^0$ $(B^+ + B^0)$

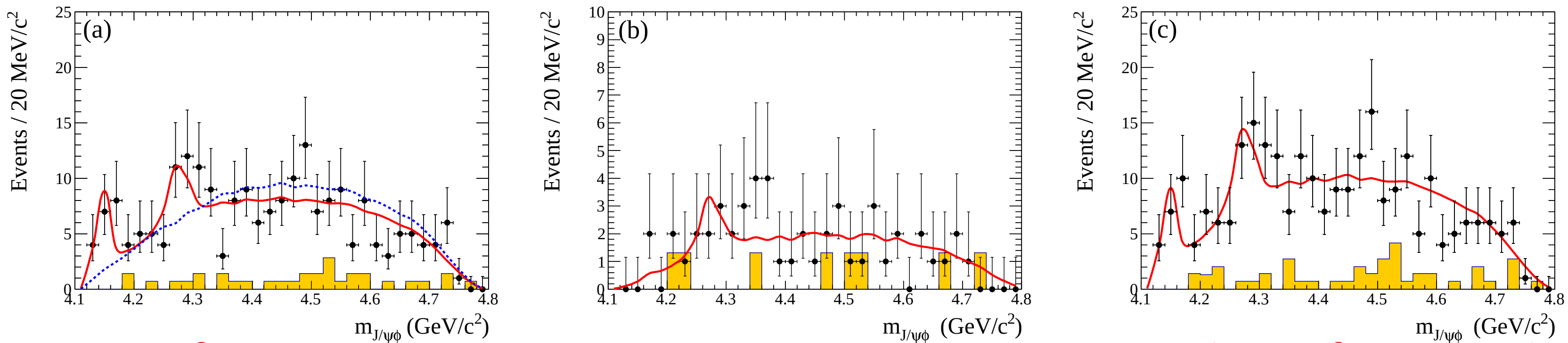


□ Fit to the $B^0$ data as a difference between the fits to the $(B^+ + B^0)$ and $B^+$ data.

□ Efficiency projection and efficiency corrected $J/\psi\phi$ mass spectrum for $(B^+ + B^0)$ data.

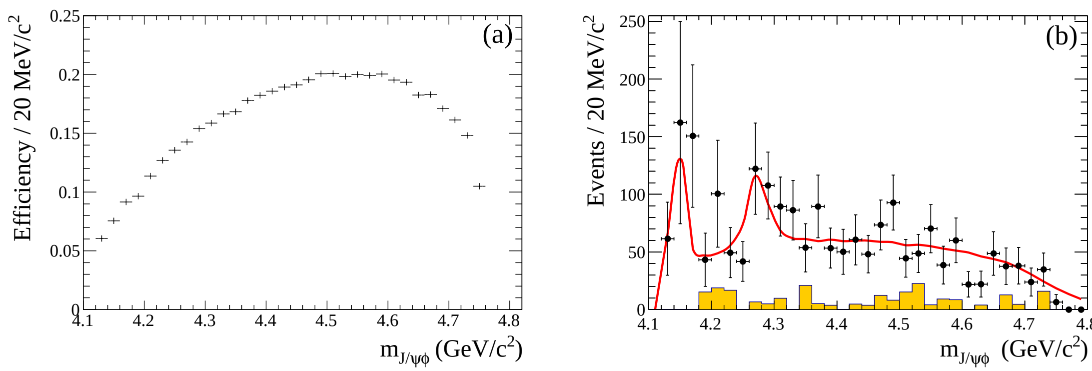

## Results from the fits.

□ Fits to the $B \to J/\psi\,\phi K$ Dalitz plot. For each fit, the table gives the fit fraction for each resonance, and the 2D and 1D $\chi^2$ values.

| Channel | $f_{X(4140)}(\%)$ | $f_{X(4270)}(\%)$ | 2D $\chi^2/\nu$ | 1D $\chi^2/\nu$ |
|---|---|---|---|---|
| $B^+$ | $9.2 \pm 3.3$ | $10.6 \pm 4.8$ | $12.7/12$ | $6.5/20$ |
| | $9.2 \pm 2.9$ | 0. | $17.4/13$ | $15.0/17$ |
| | 0. | $10.0 \pm 4.8$ | $20.7/13$ | $19.3/19$ |
| | 0. | 0. | $26.4/14$ | $34.2/18$ |
| $B^0 + B^+$ | $7.3 \pm 3.8$ | $12.0 \pm 4.9$ | $8.5/12$ | $15.9/19$ |

□ We obtain the following background-corrected fractions for $B^+$:

$$f_{X(4140)} = (9.2 \pm 3.3 \pm 4.7)\%, \;\; f_{X(4270)} = (10.6 \pm 4.8 \pm 7.1)\%$$

□ Combining statistical and systematic uncertainties in quadrature, we obtain significances of 1.6 and 1.2$\sigma$ for $X(4140)$ and $X(4270)$, respectively.

## Upper limits.

□ We obtain the ULs at 90% c.l.:

$$\mathcal{B}(B^+ \to X(4140)K^+) \times \mathcal{B}(X(4140) \to J/\psi\,\phi)/\mathcal{B}(B^+ \to J/\psi\,\phi K^+) < 0.135$$

$$\mathcal{B}(B^+ \to X(4270)K^+) \times \mathcal{B}(X(4270) \to J/\psi\,\phi)/\mathcal{B}(B^+ \to J/\psi\,\phi K^+) < 0.184$$

□ The $X(4140)$ limit may be compared with the CDF measurement of $0.149 \pm 0.039 \pm 0.024$ and the LHCb limit of 0.07.

□ The $X(4270)$ limit may be compared with the LHCb limit of 0.08.

□ Similar results are obtained using the CMS measurements.

## Conclusions.

□ We obtain first observation of new $\eta_c$ and $\eta_c(2S)$ decay modes in the $\eta K^+K^-$ and $\pi^0 K^+K^-$ produced in two-photon interactions.

□ We perform the first Dalitz plot analyses of $\eta_c$ decays to three-body. These decays are dominated by scalar meson resonances.

□ We report the first observation of $K_0^*(1430) \to K\eta$, measure its parameters and its branching fraction.

□ We obtain a new estimate of the pseudoscalars mixing angle which does not agree well with measurements obtained from the study of spin-2 resonances.

□ The isobar model for $K_0^*(1430)$ does not describe well the Dalitz plot of $\eta_c \to K^+K^-\pi^0$. Alternative models need to be tested.

# Conclusions.

□ We study the decays $B^+ \to J/\psi \phi K^+$, $B^0 \to J/\psi \phi K^0_S$ and measure new branching fractions.

□ We search for new resonances in the $J/\psi \phi$ mass spectrum from $B$ decays.

□ We find that the phase-space uniform distribution does not describe the data well.

□ We derive upper limits for the production of $X(4140)$ and $X(4270)$.